

Modeling the morphogenesis of brine channels in sea ice

B. Kutschan

Ident Technologies GmbH, Rudower Chaussee 29, 12489 Berlin, Germany

K. Morawetz

Forschungszentrum Dresden-Rossendorf, PF 51 01 19, 01314 Dresden, Germany

International Center for Condensed Matter Physics, Universidade de Brasília, 70904-910, Brasília-DF, Brazil

S. Gemming

Forschungszentrum Dresden-Rossendorf, PF 51 01 19, 01314 Dresden, Germany

Abstract. Brine channels are formed in sea ice under certain constraints and represent a habitat of different microorganisms. The complex system depends on a number of various quantities as salinity, density, pH-value or temperature. Each quantity governs the process of brine channel formation. There exists a strong link between bulk salinity and the presence of brine drainage channels in growing ice with respect to both the horizontal and vertical planes. We develop a suitable phenomenological model for the formation of brine channels both referring to the Ginzburg-Landau-theory of phase transitions as well as to the chemical basis of morphogenesis according to Turing. It is possible to conclude from the critical wavenumber on the size of the structure and the critical parameters. The theoretically deduced transition rates have the same magnitude as the experimental values. The model creates channels of similar size as observed experimentally. An extension of the model towards channels with different sizes is possible. The microstructure of ice determines the albedo feedback and plays therefore an important role for large-scale global circulation models (GCMs).

1. Introduction

Formation and decay of complex structures depend on changes in entropy. In the long run structures tend to decay, because according to *Clausius* [1867] the entropy of universe leads to a maximum, the universe evolves into a 'dead' steady state. On the other hand not only living cells avoid the global thermodynamic equilibrium. The growth period of cyclones and anticyclones or tornadoes and clouds are examples for structure formations in the so-called lifeless nature, so that the cyclogenesis shows also similarities to the animate nature. In this spirit the story book character Jonathan Leverkühn from "Doktor Faustus" by THOMAS MANN found a similar pleasure in ice crystals and reasoned that we sin against the inanimate nature, "when we draw too hard and fast a line between the two fields, since in reality it is pervious and there is no elementary capacity which is reserved entirely to the living creature and which the biologist could not also study on an inanimate subject" *Mann* [1992].

According to *Schrödinger* [1944] an organism "maintains itself" stationary at a fairly high level of order which means a fairly low level of entropy. In fact, the organisms are continually "sucking" order from their environment in the form of e.g. energy-rich food and return low-energy degradation products. *Turing* [1952] showed in his paper about the chemical basis of morphogenesis which additional conditions are necessary in order to develop a pattern or structure. For instance, the formation of cells due to an instability of the homogeneous equilibrium which is triggered off by random disturbances. Organisms delay the decay into thermodynamic equilibrium (death) by metabolism processes with

the environment, i.e. the organism succeeds in freeing itself from all the noxious entropy while alive. The working process of an entropy pump requires free energy, which leads to a minimum. The pinnate net of venation in leaves can be considered as a Turing structure too *Tyvand* [2000]. In this sense it should be possible, that the habitat of microorganisms in the polar areas, the brine channels in the sea ice, can be described through a Turing structure.

The internal surface structure of ice changes dramatically when the ice cools below -23°C or warms above -5°C and has a crucial influence on the species composition and distribution within sea ice *Light et al.* [2003]; *Kremps et al.* [2000]. This observation correlates with the change of the coverage of organisms in brine channels between -2°C and -6°C *Kremps et al.* [2000]. *Golden et al.* [1998] found a critical brine volume fraction of 5 percent, or a temperature of -5°C for salinity of 5 parts per thousand where the ice distinguishes between permeable and impermeable behavior concerning energy and nutrient transport. According to *Perovich and Gow* [1991] the brine volume increases from 2 to 37 ‰ and the correlation length increases from 0.14 to 0.22 mm if the temperature rises from -20°C to -1°C . The permeability varies over more than six orders of magnitude *Eicken* [2003]. Whereas *Golden et al.* [1998] used a percolation model we will demonstrate how the brine channel distribution can be modeled by a reaction-diffusion equation similar to the Ginzburg-Landau treatment of phase transitions. A molecular dynamics simulation shows us the change between the hexagonal arranged ice structure and the more disordered liquid water structure *Nada et al.* [2004].

After a short introduction into the key issue of the structure formation we describe a brine channel structure in sea ice and propose a phenomenological description of the problem. For the interpretation of the order parameter we discuss some microscopic properties of water using molecular dynamics simulation in the next chapter 2. In chapter 3 we consider the phase transition and the conditions which allow a structure formation. We verify the model on the basis of measured values in chapter 4 and give finally an outlook on further investigations in chapter 5.

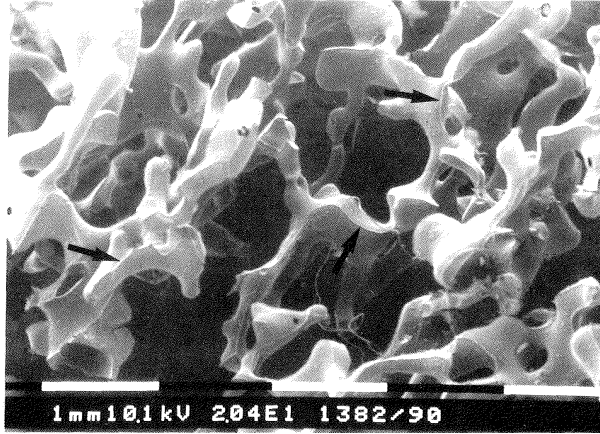


Figure 1. SEM-image of a cast of brine channels *Weissenberger* [1992].

2. Microscopic properties of water

2.1. Formation of brine channels

Various publications report on the living conditions for different organism groups in the polar areas in brine-filled holes, which arise under certain boundary conditions in sea ice as base- or brine channels (lacuna) *Bartsch* [1989]; *Trinks et al.* [2005]; *Weissenberger* [1992]. They are characterized by the simultaneous existence of different phases, water and ice in a saline environment. Because already marginal temperature variations can disturb this sensitive system, direct measurements of the salinity, temperature, pH-value or ice crystal are morphologically difficult *Weissenberger* [1992]. *Weissenberger et al.* [1992] developed a cast technique in order to examine the channel structure. Freeze-drying eliminates the ice by sublimation, and the hardened casts illustrate the channels as negative pattern. Figure 1 shows a typical granular texture without prevalent orientation.

Sometimes, both columnar and mixed textures occur. Using an imaging system *Light et al.* [2003] found brine tubes, brine pockets, bubbles, drained inclusions, transparent areas, and poorly defined inclusions. Air bubbles are much larger than brine pockets. Bubbles possess a mean major axis length of some millimeters and brine pockets are hundred times smaller *Perovich and Gow* [1996]. *Cox* [1983]; *Cox and Weeks* [1983]; *Cox* [1988] presented some quantitative model approaches, which investigated the brine channel volume, salinity profile or heat expansion but without pattern formation. They also described the texture and genetic classification of the sea ice structure experimentally. A crucial factor for the brine channel structure formation is the spatial variability of salinity *Cottier et al.* [1999].

Different mechanisms are employing the mobility of brine channels which can be used to measure the salinity profile *Cottier et al.* [1999]. Advanced micro-scale photography has been developed to observe in situ the distribution of bottom ice algae *Mundy et al.* [2007] which allows to determine the variability of the brine channel diameter from bottom to top of the ice. By mesocosm studies the hypothesis was established that the vertical brine stability is the crucial factor for ice algae growth *Krems et al.* [2001]. Therefore the channel formation during solidification and its dependence on the salinity is of great interest both experimentally and theoretically *Worster and Wettlaufer* [1997]. Experimentally *Cottier et al.* [1999] presented images, which show the

linkages between salinity and brine channel distribution in an ice sample.

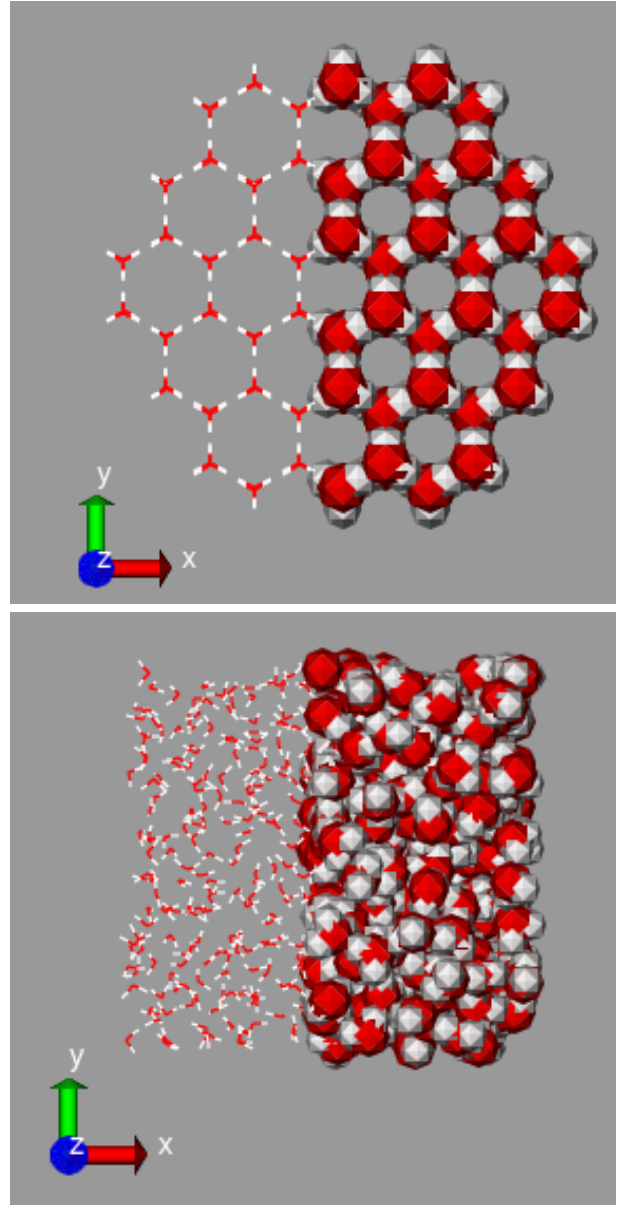


Figure 2. Hexagonal ice (above) and liquid water at 300K (below).

An approach to describe different phases in sea ice dependent on temperature and salinity relies on a reaction diffusion system

$$\frac{\partial \mathbf{w}(x, t)}{\partial t} = \mathbf{f}(x, t) + \mathbf{D} \nabla^2 \mathbf{w}(x, t), \quad (1)$$

where $\mathbf{w} = \begin{pmatrix} u \\ v \end{pmatrix}$ is the vector of reactants, $\mathbf{x} = (x, y, z)$ the three dimensional space vector, \mathbf{f} the nonlinear reaction kinetics and $\mathbf{D} = \begin{pmatrix} D_1 & 0 \\ 0 & D_2 \end{pmatrix}$ the matrix of diffusivities, where D_1 is the diffusion coefficient of water and D_2 is the diffusion coefficient of salt. For the one and two-dimensional

case we set $\mathbf{y} = \mathbf{z} = \mathbf{0}$ respectively $\mathbf{z} = \mathbf{0}$. The reaction kinetics described by $\mathbf{f}(\mathbf{x}, t)$ can include the theory of phase transitions by Ginzburg-Landau for the order parameters. Referring to this *Fabrizio* [2008] presented an ice-water phase transition. Under certain conditions, spatial patterns evolve in the so-called Turing space. The patterns reproduce the distribution of sea water with high salinity to sea ice with low salinity. The brine channel system exists below a critical temperature in a thermodynamic non-equilibrium. It is driven via the desalination of ice during the freezing process that leads to a salinity increase in the brine channels. The higher salt concentration in the remaining liquid phase leads to a freezing point depression and triggers the ocean currents.

2.2. Different states of water

Already WILHELM CONRAD RÖNTGEN had described the anomalous properties of water with molecules of the first kind, which he called ice molecules and molecules of the second kind *Röntgen* [1892] and which represent the liquid aggregate state. *Dennison* [1921] determined the ordinary hexagonal ice-I modification from X-ray pattern methodically verified by *Bragg* [1922]. This so called E_h -ice is formed by four oxygen atoms which build a tetrahedron as illustrated in figure 2. In E_h -ice each oxygen atom is tetrahedrally coordinated by four neighbouring oxygen atoms, each coordinated by a hydrogen bridge. The arrangement is isomorphous with the wurtzite form of zinc sulphide or with the silicon atoms in the tridymite form of silicon dioxide. *Bjerrum* [1951] and *Eisenberg and Kauzmann* [2005] provided a survey about the structure differences between the different polymorphic forms of ice and liquid water.

Molecular dynamics simulations with the TIP3P-model of water using the NAMD-software of the Theoretical and Computational Biophysics Group of the university of Illinois show the change from a regular hexagonal lattice structure to irregular bonds after the melting (figure 2). *Nada et al.* [2004] developed a better six-site potential model of H_2O for a crystal growth of ice from water using molecular dynamics and Monte Carlo methods. They computed both the free energy and an order parameter for the description of the water structure. Also *Medvedev and Naberukhin* [1987] introduced a "tetrahedrality measure" M_T for the ordering degree of water. So it is possible to discriminate between ice- and water molecules via a two-state function ($G = 0$ if $M_T \geq M_T^c$ and $G = 1$ if $M_T < M_T^c$). This tetrahedrality is computed using the sum

$$M_T = \frac{1}{15 < l^2 >} \sum_{i,j} (l_i - l_j)^2, \quad (2)$$

where l_i are the lengths of the six edges of the tetrahedron formed by the four nearest neighbors of the considered water molecule. For an ideal tetrahedron one has $M_T = 0$ and the random structure yields $M_T = 1$. The tetrahedrality can be used in order to define an order parameter according to the Landau - de Gennes model for liquid crystals, which refers to the Clausius-Mosotti-relation. Other simulations such as the percolation models of *Stanley* [1979]; *Stanley and Teixeira* [1980] use a two-state model, in which a critical correlation length determines the phase transition. A mesoscopic model for the sea ice crystal growth are developed by *Kawano and Ohashi* [2009] who used a Voronoi dynamics.

3. Model equations

3.1. One-dimensional case

We consider a reaction diffusion system

$$\frac{\partial u(x,t)}{\partial t} = a_1 u - cu^3 + du^5 + b_1 v + D_1 \frac{\partial^2 u(x,t)}{\partial x^2} \quad (3)$$

$$\frac{\partial v(x,t)}{\partial t} = -a_2 v - b_2 u + D_2 \frac{\partial^2 v(x,t)}{\partial x^2} \quad (4)$$

in one space dimension. Let $u(x,t)$ be the order parameter according to the Ginzburg-Landau-theory with $u_{min} \leq u_c \leq u_{max}$ and u is proportional to the tetrahedrality M_T , $u \sim M_T$. If the variable u is smaller than u_c ($u < u_c$), the phase changes from water to ice and vice versa. Thus, changes in u reflect temperature variations. The variable v is a measure of the salinity. The coefficient a_1 depends on the temperature T as $(T - T_c)/T_c$ with the critical temperature T_c . The salt exchange between ice and water is realized by the gain term $b_1 v$ and the loss term $-a_2 v$. The positive terms $a_1 u$ and $b_1 v$ are the temperature- and salt-concentration-dependent "driving forces" of the system.

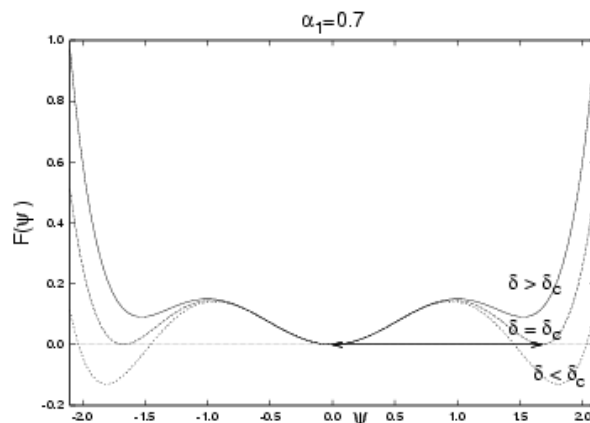


Figure 3. Landau-function (9) versus the dimensionless order parameter (tetrahedrality) for various δ .

In order to realize the T -dependent phase transition, one can expand the order parameter in a power series corresponding to Ginzburg and Landau in equation 3. In order to describe properly a temperature-induced phase transition of second order an expression $-cu^3$ is necessary. The first-order phase transition is dependent on du^5 . Supercooled or superheated phases can coexist, i.e. an hysteresis behavior is possible. We write the equations (3) and (4) in dimensionless form (see appendix) by setting $\tau = \sqrt{b_1 b_2} t$, $\xi = \sqrt[4]{b_1 b_2 / D_1^2} x$, $\psi = \sqrt[4]{c^2 / b_1 b_2} u$, $\rho = \sqrt[4]{b_1 c^2 / b_2^3} v$ and get

$$\frac{\partial \psi(\xi, \tau)}{\partial \tau} = f[\psi, \rho] + \frac{\partial^2 \psi(\xi, \tau)}{\partial \xi^2} \quad (5)$$

$$\frac{\partial \rho(\xi, \tau)}{\partial \tau} = g[\psi, \rho] + D \frac{\partial^2 \rho(\xi, \tau)}{\partial \xi^2} \quad (6)$$

with $\alpha_1 = a_1 / \sqrt{b_1 b_2}$, $\delta = d \sqrt{b_1 b_2} / c^2$, $\alpha_2 = a_2 / \sqrt{b_1 b_2}$ and $D = D_2 / D_1$ as well as the reaction kinetics

$$f[\psi, \rho] = \alpha_1 \psi - \psi^3 + \delta \psi^5 + \rho \quad (7)$$

$$g[\psi, \rho] = -\alpha_2 \rho - \psi, \quad (8)$$

where ψ is the dimensionless order parameter of the water/ice system and ρ the dimensionless salinity. Thus the dynamics only depends on four parameters α_1 , α_2 , δ and D . Without the salinity ρ in equation (3) respectively (5) the above equation system is reduced to a Ginzburg-Landau equation for phase transitions of first order.

3.1.1. First Order Phase Transitions

When we neglect the salinity ρ , the integration of the kinetic function (7) yields the Landau function for the order parameter ψ of water/ice

$$F = \frac{a_1}{2}\psi^2 - \frac{1}{4}\psi^4 + \frac{\delta}{6}\psi^6 \quad (9)$$

as plotted in figure 3. It possesses three minima

$$\psi_{\min} = \left\{ 0, \pm \sqrt{\frac{1}{2\delta} \left(1 + \sqrt{1 - 4\delta\alpha_1} \right)} \right\}. \quad (10)$$

The values are given in figure 3. When several different minima of equal depth exist, then there is a discontinuity in ψ and one has a first-order phase transition. This is the case if

$$\delta = \delta_c = \frac{3}{16\alpha_{1c}}. \quad (11)$$

Thus the critical parameter $\delta = \delta_c$ is determined by the temperature-dependent critical value $\alpha_1 = \alpha_{1c}$. The jump in figures 3 and 4 is a measure for the latent heat of the phase transition from water to ice. *Feistel and Hagen* [1998] deduced theoretically the latent heat of sea ice for various salinities.

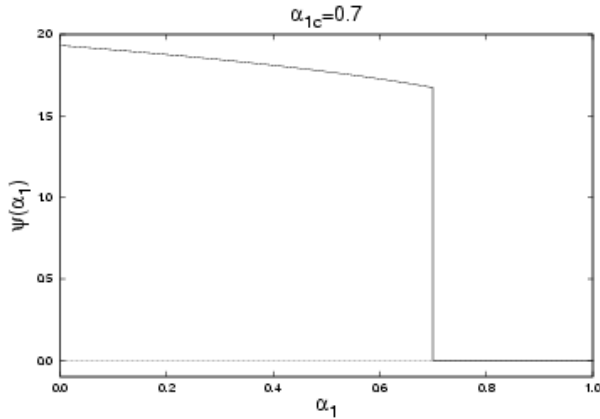


Figure 4. The minimal order parameter ψ_{\min} of (10) dependent on α_1 .

3.1.2. Linear Stability Analysis

First we perform a linear stability analysis by linearizing the equation system (5) and (6) according to $\psi = \psi_0 + \bar{\psi}$ and $\rho = \rho_0 + \bar{\rho}$. We obtain the characteristic equation for the fix points with $\bar{\psi} = \psi_i \exp(\lambda\tau + i\kappa\xi)$ and $\bar{\rho} = \rho_i \exp(\lambda\tau + i\kappa\xi)$, see appendix, as

$$\begin{pmatrix} \frac{\partial}{\partial \tau} \bar{\psi} \\ \frac{\partial}{\partial \tau} \bar{\rho} \end{pmatrix} = \begin{pmatrix} \alpha_1 - 3\psi_0^2 + 5\delta\psi_0^4 & 1 \\ -1 & -\alpha_2 \end{pmatrix} \begin{pmatrix} \bar{\psi} \\ \bar{\rho} \end{pmatrix} + \begin{pmatrix} \frac{\partial^2}{\partial \xi^2} & 0 \\ 0 & D \frac{\partial^2}{\partial \xi^2} \end{pmatrix} \begin{pmatrix} \bar{\psi} \\ \bar{\rho} \end{pmatrix}. \quad (12)$$

There are five fix points for the kinetics (7) and (8) which satisfy $f = 0$ and $g = 0$. In order to get a stable non-oscillating pattern we need a stable spiral point as fix point. Moreover the associated eigenvalues have to possess a positive real part for a positive wavenumber, i.e. they have to allow to create unstable modes (fig. 5). Not each fix point satisfies both conditions. Therefore for the following discus-

ion we choose the steady state, $\psi_0 = 0$ and $\rho_0 = 0$, which corresponds to the observable brine channel structures measured by a casting experiment *Mundy et al.* [2007]; *Cottier et al.* [1999].

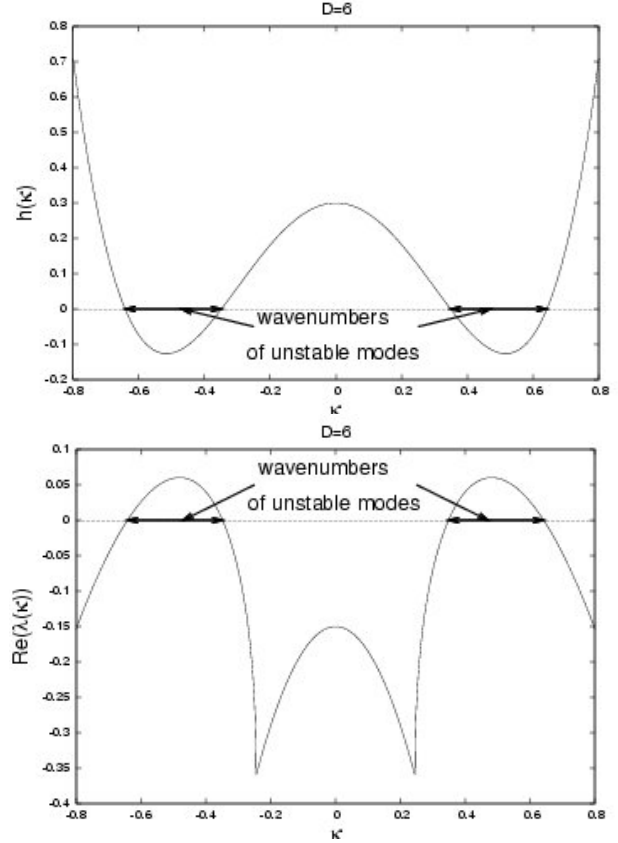


Figure 5. Dispersion of the linear stability (13) and (14) versus the dimensionless wave number κ for $\alpha_1 = 0.7$, $\alpha_2 = 1$, $D = 6$.

Short-time experiments may also record structures that are formed under non-steady conditions. Since those structures are beyond the scope of the present paper, we proceed with the steady state which leads to

$$\lambda^2 + [\kappa^2(1+D) + \alpha_2 - \alpha_1]\lambda + h(\kappa^2) = 0 \quad (13)$$

with

$$h(\kappa^2) = D\kappa^4 + (\alpha_2 - \alpha_1 D)\kappa^2 - \alpha_1\alpha_2 + 1. \quad (14)$$

Both equations are easily solved for λ as plotted in fig. 5 for critical wavenumbers κ_c . The critical wavenumber can be found from the largest modes. These are given by the minimum of equation (14) from which we find the wavenumbers

$$\kappa_{min}^2 = \frac{1}{2D}(Df_\psi + g_\rho) = \frac{1}{2D}(D\alpha_1 - \alpha_2) \quad (15)$$

and the minima

$$h_{min} = f_\psi g_\rho - g_\psi f_\rho - \frac{(Df_\psi + g_\rho)^2}{4D} = 1 - \frac{(D\alpha_1 + \alpha_2)^2}{4D}. \quad (16)$$

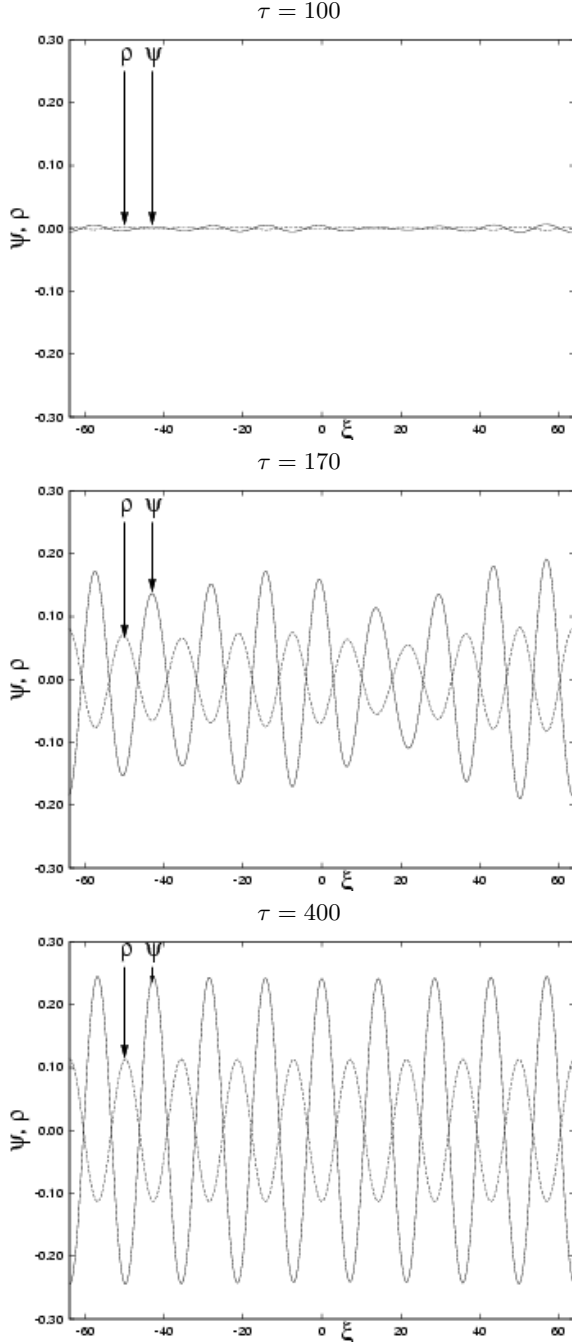


Figure 6. Snapshots of the time evolution of the order parameter ψ and salinity ρ versus spatial coordinates showing a structure formation for $\alpha_1 = 0.7$, $\alpha_2 = 1$, $\delta = \frac{3}{16\alpha_1}$, $D = 6$ with the initial condition $\rho(\tau = 0) = 0.5 \pm 0.01N(0, 1)$ and periodic boundary conditions.

The formation of a spatial Turing structure, a non-oscillating pattern, requires a non-positive h_{min} for $\kappa_{min}^2 > 0$. In this case there is a range of wavenumbers which are linearly unstable (fig. 5). This can be obtained, if the diffusion coefficient D is greater than the critical diffusion coefficient D_c

$$D_c = -\frac{\alpha_1\alpha_2 - 2}{\alpha_1^2} + \frac{2}{\alpha_1^2}\sqrt{1 - \alpha_1\alpha_2}, \quad (17)$$

which we get from $h_{min} = 0$ with the critical wavenumber κ_c

$$\kappa_c^2 = -\frac{D_c f_\psi + g_\rho}{2D_c} = \frac{D_c\alpha_1 + \alpha_2}{2D_c}. \quad (18)$$

The size of the structure can be estimated from $\frac{2\pi}{\kappa_c}$. The pattern size depends on the three parameters α_1 , α_2 and D . The three parameters determine the brine channel size and vice versa. With the parameters chosen in fig. 5 we obtain a pattern size of 12.2. In the next chapter we compare this value with experimental quantities. With a small initial random perturbation we plot snapshots of the time evolution of the order parameter ψ and the salinity ρ in figure 6. The quantities ψ and ρ are opposite to each other; domains with low salinity correspond to domains with ice and vice versa. We see the formation of a mean mode given by the wave length κ_c . For $\kappa_c = 0$ a homogeneous phase is formed. Thus the Turing space is bounded by $h(\kappa^2) \leq 0$. If we restrict the discussion to spatial homogeneity, $\kappa = 0$, the fix points $\psi = 0$ and $\rho = 0$ are stable according to the eigenvalues (13),

$$\lambda_{1,2} = -\frac{\alpha_2 - \alpha_1}{2} \pm \frac{1}{2}\sqrt{(\alpha_1 + \alpha_2)^2 - 4}, \quad (19)$$

for $\alpha_2 > \alpha_1$ and $\alpha_1\alpha_2 < 1$. The trajectories of salinity ρ and the order parameter ψ converge to the steady state value zero by damped oscillation as seen in figure 7.

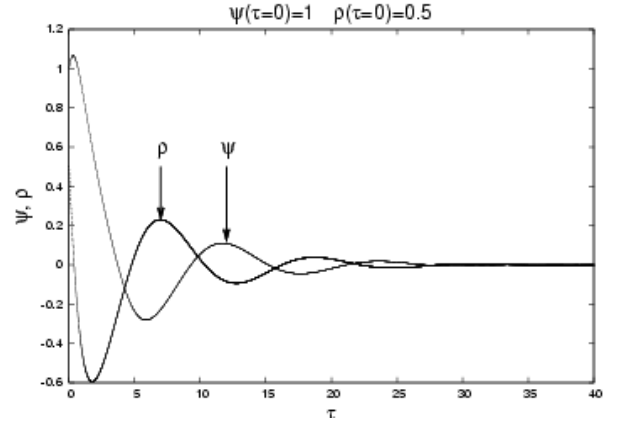


Figure 7. Time evolution of the order parameter ψ and the salinity ρ for $\alpha_1 = 0.7$, $\alpha_2 = 1$, $\delta = \frac{3}{16\alpha_1}$ and the initial order parameter $\psi(\tau = 0) = 1$ and the dimensionless salinity $\rho(\tau = 0) = 0.5$.

3.2. Two-dimensional case

From the characteristic equation in the two-dimensional case

$$\lambda^2 + [(\kappa_\xi^2 + \kappa_\eta^2)(1 + D) + \alpha_2 - \alpha_1]\lambda + h(\kappa_\xi^2, \kappa_\eta^2) = 0 \quad (20)$$

we find the corresponding dispersion relation illustrated in figure 8

$$h(\kappa_\xi^2, \kappa_\eta^2) = D(\kappa_\xi^2 + \kappa_\eta^2)^2 + (\alpha_2 - \alpha_1 D)(\kappa_\xi^2 + \kappa_\eta^2) - \alpha_1\alpha_2 + 1. \quad (21)$$

The Turing space is bounded by the sectional plane $h = 0$. The evolution of the order parameter ψ and the salinity ρ is illustrated in figures 9 and 10. Their behavior is inversely proportional and corresponds to the fact, that a high salinity occurs in the water phase and a low salinity in the ice phase. The model kinetics generate brine channels of similar

size. In order to obtain a hierarchical net of brine channels of different size, the kinetics in the basic equations can be changed *Murray* [1993].

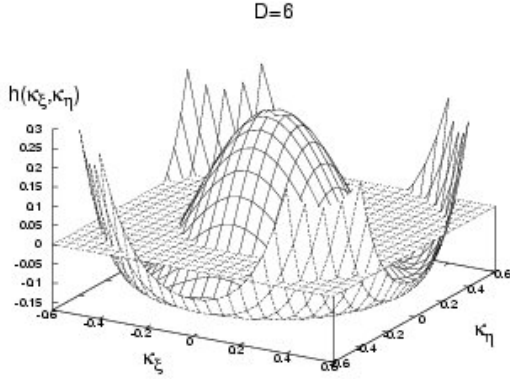


Figure 8. Dispersion of the two-dimensional characteristics (20) and (21) for $\alpha_1 = 0.7$, $\alpha_2 = 1$, $D = 6$.

4. Connection to experimental data

The critical domain size is determined by the equation (18). Due to this relation we can infer other parameters in the model equations (3) and (4). From the relation between the dimensionless wavenumber κ and the dimensional wavenumber k

$$\kappa^2 = \frac{\alpha_1 D - \alpha_2}{2D} = \frac{D_1}{\sqrt{b_1 b_2}} k^2 \quad (22)$$

we get

$$\frac{2\pi}{\kappa_c} = 12.2 = \frac{2\pi}{k_c} \frac{\sqrt[4]{b_1 b_2}}{\sqrt{D_1}}. \quad (23)$$

The observed diameters of the brine channels range from μm to mm scale *Weissenberger* [1992]. For a size of $2\pi/k_c = 10\mu\text{m}$ and a diffusion coefficient $D_1 = 10^{-5} \text{cm}^2 \text{s}^{-1}$ for H_2O -molecules we obtain the product $b_1 b_2 = 2.2 \cdot 10^6 \text{s}^{-2}$ and a transition rate $a_1 = \sqrt{b_1 b_2} \alpha_1 = 1042 \text{s}^{-1}$. The rate a_1 is proportional to the reorientations of the molecules per second, $1/\tau_d = 10^5 \text{s}^{-1}$ *Eisenberg and Kauzmann* [2005] and to the scaled temperature $\frac{T_c - T}{T_c}$

$$a_1 \sim \frac{T_c - T}{T_c} \frac{1}{\tau_d}, \quad (24)$$

where T_c is the melting point depending on the salinity. The mean salinity in sea ice of 35g/l corresponds to 1 NaCl -molecule at 100 H_2O -molecules, i.e. 1 Na^+ -ion and 1 Cl^- -ion at 100 H_2O -molecules in a diluted solution after the dissociation, thus a ratio of $x = (n_{\text{Na}^+} + n_{\text{Cl}^-})/n_{\text{H}_2\text{O}} = 1/50$. From that condition we obtain according to Clausius-Clapeyron

$$\Delta T = - \frac{xRT^2}{\Delta H} \quad (25)$$

a freezing point depression from 0°C to -2°C , where $\Delta H = 6 \frac{\text{kJ}}{\text{mol}}$ is the latent heat for the phase transition from water to ice, $R = 8.314 \frac{\text{J}}{\text{molK}}$ is the universal gas constant and $T = 273\text{K}$. Thus we get correctly $T_c = 271\text{K}$. For an en-

vironment temperature of $T = -5^\circ\text{C} = 268\text{K}$ according to (24), a transition rate of $\frac{268-271}{271} \cdot 10^5 \text{s}^{-1} = 1107 \text{s}^{-1}$ follows which nearly corresponds to $a_1 = 1042 \text{s}^{-1}$, which we estimated from the domain size (22).

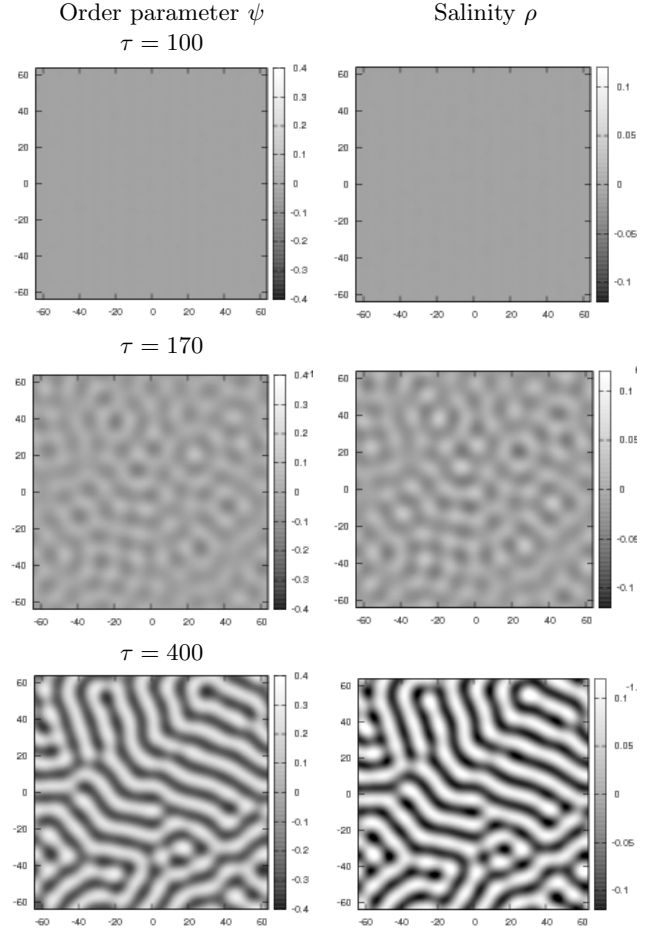


Figure 9. Structure formation for 3 time steps $\tau = 100, 170, 400$ (from top to bottom) for $a_1 = 0.7$, $a_2 = 1$, $d = \frac{3}{16a_1}$, $D = 6$ with the initial condition $v(t=0) = 0.5 \pm 0.01N(0, 1)$ and periodic boundary conditions.

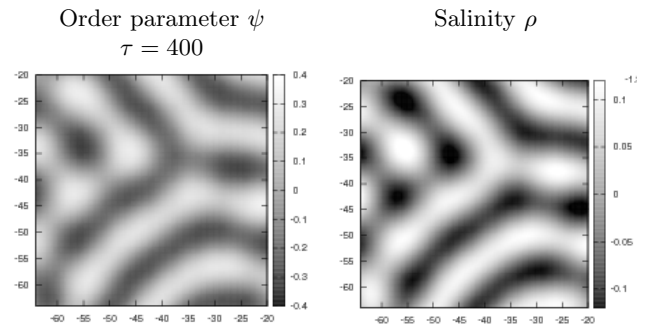


Figure 10. Magnification of a detail of figure 9.

Furthermore we find the transition rate $a_2 = \sqrt{b_1 b_2} \alpha_2 = 1483 \text{s}^{-1}$ and the diffusion coefficient $D_2 = 6 \times 10^{-5} \frac{\text{cm}^2}{\text{s}}$. Due to the transformation of equation (3) into a dimension-

less form (5) there exists a fixed relation (11) because of $c = 1$. We obtain for the equation (3) the rate d_c with $\alpha_1 = a_1/\sqrt{b_1 b_2}$, $\delta = d\sqrt{b_1 b_2}/c^2$ of

$$d_c = \frac{3c^2}{16a_1}, \quad (26)$$

which is proportional to c^2 .

5. Conclusion

In this paper it has been shown that a reaction diffusion system which connects the basic ideas both of Ginzburg and of Turing can describe the formation of brine channels with realistic parameters. For the chosen parameters patterns of similar size emerged. This fact follows from the dispersion as shown in fig. 5 and 8. *Eicken* [1991] and *Weissenberger* [1992] distinguished between six various texture classes of sea ice dependent on the crystal morphology, brine inclusions and the genesis. The different ice crystal growth depends on snow deposition, flooding, turbulent mixing, quiescent growth rate or supercooling. Each condition determines the character of kinetics. Non-linear heat and salt dissipation for example leads to dendritic growth (snowflakes) whereas one observes in sea ice mostly lamellar or cellular structures rather than completely dendritic *Eicken* [2003]. Hence, the morphology of sea ice is one criterion for the choice of an appropriate kinetics for the genesis of sea ice. Therefore, in order to simulate different structur sizes and textures, we can modify the dispersion relation by variation of the parameters α_1 , α_2 and D or by a modified kinetics *Turk* [1991]. The crucial point is the shape of the dispersion function. If there are multiple different positive unstable regions for the wavenumbers with positive real part of eigenvalues we could expect that differently large channels evolve. For instance *Worster and Wettlaufer* [1997] presented a general theory for convection with mushy layers. The two different minima of the neutral curve, determines by a linear stability analysis, correspond to two different modes of convection, which affect the kinetics and as a consequence of this the size distribution of the brine channels. We note that the initial conditions are decisive for the appearance of specific patterns *Murray* [1993]. Hence one should investigate how dislocations or antifreeze proteins influence the formation of the brine channel distribution.

6. Appendix

6.1. Dimensionless Quantities

If we set $\tau = \frac{t}{t_0}$, $\xi = \frac{x}{x_0}$, $u = C_1\psi$ and $v = C_2\rho$ we get with $\frac{\partial\psi}{\partial t} = \frac{\partial\tau}{\partial t} \frac{\partial\psi}{\partial\tau} = \frac{1}{t_0} \frac{\partial\psi}{\partial\tau}$ and $\frac{\partial\psi}{\partial x} = \frac{\partial\xi}{\partial x} \frac{\partial\psi}{\partial\xi} = \frac{1}{x_0} \frac{\partial\psi}{\partial\xi}$

$$\frac{\partial u}{\partial t} = C_1 \frac{\partial\psi}{\partial t} = \frac{C_1}{t_0} \frac{\partial\psi}{\partial\tau} \quad (27)$$

and

$$\frac{\partial u}{\partial x} = C_1 \frac{\partial\psi}{\partial x} = \frac{C_1}{x_0} \frac{\partial\psi}{\partial\xi}. \quad (28)$$

Because of $\frac{\partial^2\psi}{\partial\xi^2} = \frac{\partial^2\psi}{\partial x^2} \left(\frac{\partial x}{\partial\xi}\right)^2 + \frac{\partial\psi}{\partial x} \frac{\partial^2 x}{\partial\xi^2} = x_0^2 \frac{\partial^2\psi}{\partial x^2}$ we obtain $\frac{\partial^2\psi}{\partial x^2} = \frac{1}{x_0^2} \frac{\partial^2\psi}{\partial\xi^2}$ and consequently

$$\frac{\partial^2 u}{\partial x^2} = C_1 \frac{\partial^2\psi}{\partial x^2} = \frac{C_1}{x_0^2} \frac{\partial^2\psi}{\partial\xi^2}. \quad (29)$$

Accordingly we obtain

$$\frac{\partial v}{\partial t} = \frac{C_2}{t_0} \frac{\partial\rho}{\partial\tau}$$

$$\frac{\partial^2 v}{\partial x^2} = \frac{C_2}{x_0^2} \frac{\partial^2\rho}{\partial\xi^2}. \quad (30)$$

From (3, 4) we get the dimensionless equations

$$\frac{\partial\psi}{\partial\tau} = f[\psi, \rho] + D_1 \frac{t_0}{x_0^2} \frac{\partial^2\psi}{\partial\xi^2} \quad (31)$$

$$\frac{\partial\rho}{\partial\tau} = g[\psi, \rho] + D_2 \frac{t_0}{x_0^2} \frac{\partial^2\rho}{\partial\xi^2} \quad (32)$$

with

$$\begin{aligned} f[\psi, \rho] &= a_1 t_0 \psi - c t_0 C_1^2 \psi^3 + d t_0 C_1^4 \psi^5 + b_1 t_0 \frac{C_2}{C_1} \rho \\ g[\psi, \rho] &= -a_2 t_0 \rho - b_2 t_0 \frac{C_1}{C_2} \psi. \end{aligned} \quad (33)$$

If we choose

$$\begin{aligned} c t_0 C_1^2 &= 1, & b_1 t_0 \frac{C_2}{C_1} &= 1, \\ D_1 \frac{t_0}{x_0^2} &= 1, & b_2 t_0 \frac{C_1}{C_2} &= 1 \end{aligned} \quad (34)$$

we obtain $C_1 = \sqrt[4]{\frac{b_1 b_2}{c^2}}$, $C_2 = \sqrt[4]{\frac{b_2^3}{b_1 c^2}}$, $t_0 = \frac{1}{\sqrt{b_1 b_2}}$ and $x_0 = \sqrt[4]{\frac{D_1^2}{b_1 b_2}}$.

6.2. Linear Stability Analysis

Let $\bar{\psi}$ and $\bar{\rho}$ denote small displacements from the equilibrium values ψ_0 and ρ_0 and write $\psi = \psi_0 + \bar{\psi}$ and $\rho = \rho_0 + \bar{\rho}$.

With respect to (5, 6) we obtain

$$\begin{aligned} \bar{\psi}_\tau(\xi, \tau) &= \alpha_1(\psi_0 + \bar{\psi}) - (\psi_0 + \bar{\psi})^3 \\ &\quad + \delta(\psi_0 + \bar{\psi})^5 + \rho_0 + \bar{\rho} + \bar{\psi}\xi\xi(\xi, \tau) \\ \bar{\rho}_\tau(\xi, \tau) &= -\alpha_2(\rho_0 + \bar{\rho}) - (\rho_0 + \bar{\rho}) + D\bar{\rho}\xi\xi(\xi, \tau). \end{aligned} \quad (35)$$

If we consider only linear terms

$$\begin{aligned} \bar{\psi}_\tau(\xi, \tau) &= \dots + \alpha_1 \bar{\psi} - 3\psi_0^2 \bar{\psi} \\ &\quad + 5\delta\psi_0^4 \bar{\psi} + \bar{\rho} + \dots + \bar{\psi}\xi\xi(\xi, \tau) \\ \bar{\rho}_\tau(\xi, \tau) &= \dots - \bar{\rho} - \alpha_2 \bar{\rho} + \dots + D\bar{\rho}\xi\xi(\xi, \tau) \end{aligned} \quad (36)$$

we get

$$\begin{aligned} \begin{pmatrix} \frac{\partial}{\partial\tau} \bar{\psi} \\ \frac{\partial}{\partial\tau} \bar{\rho} \end{pmatrix} &= \underbrace{\begin{pmatrix} \alpha_1 - 3\psi_0^2 + 5\delta\psi_0^4 & 1 \\ -1 & -\alpha_2 \end{pmatrix}}_{J_{(\psi=\psi_0, \rho=\rho_0)}} \begin{pmatrix} \bar{\psi} \\ \bar{\rho} \end{pmatrix} \\ &\quad + \begin{pmatrix} \frac{\partial^2}{\partial\xi^2} & 0 \\ 0 & D \frac{\partial^2}{\partial\xi^2} \end{pmatrix} \begin{pmatrix} \bar{\psi} \\ \bar{\rho} \end{pmatrix}, \end{aligned} \quad (37)$$

where $J_{(\psi=\psi_0, \rho=\rho_0)}$ is the Jacobian

$$\begin{aligned} J_{(\psi=\psi_0, \rho=\rho_0)} &= \begin{pmatrix} f_\psi & f_\rho \\ g_\psi & g_\rho \end{pmatrix}_{(\psi=\psi_0, \rho=\rho_0)} \\ &= \begin{pmatrix} \alpha_1 - 3\psi_0^2 + 5\delta\psi_0^4 & 1 \\ -1 & -\alpha_2 \end{pmatrix}, \end{aligned} \quad (38)$$

which we can calculate also considering (7, 8).

If we set the Fourier ansatz $\bar{\psi} = \psi_0 \exp(\lambda\tau + i\kappa\xi)$ and $\bar{\rho} = \rho_0 \exp(\lambda\tau + i\kappa\xi)$ in (12) we find

$$\begin{pmatrix} \lambda\bar{\psi}_i \\ \lambda\bar{\rho}_i \end{pmatrix} = \begin{pmatrix} \alpha_1 - 3\psi_0^2 + 5\delta\psi_0^4 & 1 \\ -1 & -\alpha_2 \end{pmatrix} \begin{pmatrix} \bar{\psi}_i \\ \bar{\rho}_i \end{pmatrix} + \begin{pmatrix} -\kappa^2 & 0 \\ 0 & -D\kappa^2 \end{pmatrix} \begin{pmatrix} \bar{\psi}_i \\ \bar{\rho}_i \end{pmatrix}. \quad (39)$$

With $\psi_0 = 0$ and $\rho_0 = 0$ we obtain the eigenvalue equation

$$\begin{pmatrix} 0 \\ 0 \end{pmatrix} = \left[\begin{pmatrix} \alpha_1 - \kappa^2 & 1 \\ -1 & -\alpha_2 - D\kappa^2 \end{pmatrix} - \begin{pmatrix} \lambda & 0 \\ 0 & \lambda \end{pmatrix} \right] \begin{pmatrix} \bar{\psi}_i \\ \bar{\rho}_i \end{pmatrix} \quad (40)$$

with the characteristic equation

$$\begin{aligned} 0 &= \begin{vmatrix} \alpha_1 - \kappa^2 - \lambda & 1 \\ -1 & -\alpha_2 - D\kappa^2 - \lambda \end{vmatrix} \\ &= \lambda^2 + [\kappa^2(1 + D) + \alpha_2 - \alpha_1]\lambda \\ &+ \underbrace{D\kappa^4 + (\alpha_2 - \alpha_1 D)\kappa^2 - \alpha_1\alpha_2 + 1}_{h(\kappa^2)}. \end{aligned} \quad (41)$$

Acknowledgments.

The authors are deeply indebted Jürgen Weissenberger for the many exposures of casts brine channels. Dr. L. Dinkel and Dr. P. Augustin are thanked for their system theoretic discussion and Dr. U. Menzel at the Rudbeck laboratory, Uppsala, Sweden for his support. This work was supported by DFG Priority Program 1157 via GE1202/06, the BMBF and by European ESF program NES. The financial support by the Brazilian Ministry of Science and Technology is acknowledged.

References

- Bartsch, A., Die Eisalgenflora des Weddellmeeres (Antarktis): Artenzusammensetzung und Biomasse sowie ökophysiologie ausgewählter Arten (sea ice algae of the weddell sea (antarctica): Species composition, biomass, and ecophysiology of selected species), *Ber. Polarforschung*, *63*, 1, 1989.
- Bjerrum, N., Structure and properties of ice, *Det Kongelige Danske Videnskabernes Selskab, Matematisk-fysiske Meddelelser*, *27*(1), 1, 1951.
- Bragg, W. H., The crystal structure of ice, *Proc. Roy. Soc. London*, *34*, 98, 1922.
- Clausius, R., *Über den zweiten Hauptsatz der mechanischen Wärmetheorie*, Friedrich Vieweg und Sohn, Braunschweig, 1867.
- Cottier, F., H. Eicken, and P. Wadhams, *J. Geophys. Res.*, *104*(C7), 15,859, 1999.
- Cox, G. F. N., Thermal expansion of saline ice, *J. Glaciol.*, *29*(103), 425, 1983.
- Cox, G. F. N., Numerical simulations of the profile properties of undeformed first-year sea ice during the growth season, *J. Geophys. Res.*, *93*, 449, 1988.
- Cox, G. F. N., and W. F. Weeks, Equations for determining the gas and brine volumes in sea-ice samples, *J. Glaciol.*, *29*(103), 306, 1983.
- Dennison, D. M., The crystal structure of ice, *Phys. Rev.*, *17*, 20, 1921.
- Eicken, H., Quantifizierung von Meereiseigenschaften: Automatische Bildanalyse von Dünnschnitten und Parametrisierung von Chlorophyll- und Salzgehaltsverteilungen (quantification of sea-ice properties: Automated image analysis of thin sections and parametrization of chlorophyll and salinity distributions), *Ber. Polarforschung*, *82*, 1, 1991.
- Eicken, H., From the microscopic, to the macroscopic, to the regional scale: Growth, microstructure and properties of sea ice,

in *Sea Ice: an introduction to its physics, chemistry, biology and geology*, edited by D. N. Thomas and G. S. Dieckmann, chap. 2, Blackwell Science Ltd, Oxford, 2003.

- Eisenberg, D., and W. Kauzmann, *The structure and properties of water*, Clarendon Press, Oxford, 2005.
- Fabrizio, M., Ice-water and liquid-vapor phase transitions by a ginzburg-landau model, *J. Math. Phys.*, *49*, 102,902, 2008.
- Feistel, R., and E. Hagen, A gibbs thermodynamic potential of sea ice, *Cold Reg. Sci. Technol.*, *28*, 83, 1998.
- Golden, K. M., S. F. Ackley, and V.I.Lytle, The percolation phase transition in sea ice, *Science*, *282*, 2238, 1998.
- Kawano, Y., and T. Ohashi, A mesoscopic numerical study of sea ice crystal growth and texture development, *Cold Reg. Sci. Technol. (Accepted date: 2 February 2009)*, 2009.
- Krembs, C., G. R., and M. Spindler, *J. Exp. Mar. Biol. Ecol.*, *243*, 55, 2000.
- Krembs, C., T. Mock, and R. Gradinger, *Polar. Biol.*, *24*, 356, 2001.
- Light, B., G. A. Maykut, and T. C. Grenfell, Effects of temperature on the microstructure of first-year arctic sea ice, *J. Geophys. Res.*, *108*, 3051, 2003.
- Mann, T., *Doktor Faustus*, Fisher Taschenbuch Verlag, 1992.
- Medvedev, N. N., and Y. I. Naberukhin, Shape of the delaunay simplices in dense random packings of hard and soft spheres, *J. Non-Cryst. Solids*, *94*, 402, 1987.
- Mundy, C. J., D. G. Barber, C. Michel, and R. F. Marsden, *Polar. Biol.*, *30*, 1099, 2007.
- Murray, J. D., *Mathematical Biology*, Springer Verlag, Berlin, 1993.
- Nada, H., J. P. van der Eerden, and Y. Furukawa, A clear observation of crystal growth of ice from water in a molecular dynamics simulation with a six-site potential model of H_2O , *J. Cryst. Growth*, *266*, 297, 2004.
- Perovich, D. K., and A. J. Gow, A statistical description of the microstructure of young sea ice, *J. Geophys. Res.*, *96*(C9), 16,943, 1991.
- Perovich, D. K., and A. J. Gow, A quantitative description of sea ice inclusions, *J. Geophys. Res.*, *101*(C8), 16,943, 1996.
- Röntgen, W. C., Über die Constitution des flüssigen Wassers, *Ann. Phys. (Leipzig)*, *45*, 91, 1892.
- Schrödinger, E., *What is Life?*, Cambridge University Press, Cambridge, 1944.
- Stanley, H. E., A polychromatic correlated-site percolation problem with possible relevance to the unusual behaviour of supercooled H_2O and D_2O , *L. Phys. A: Math. Gen.*, *12*, L329, 1979.
- Stanley, H. E., and J. Teixeira, Interpretation of the unusual behavior of H_2O and D_2O at low temperatures: Tests of a percolation model, *J. Chem. Phys.*, *73*, 3404, 1980.
- Trinks, H., W. Schröder, and C. K. Biebricher, Ice and the origin of life, *Origins Life Evol. Biosphere*, *35*, 429, 2005.
- Turing, A. M., The chemical basis of morphogenesis, *Phil. Trans. of the R. Soc. B: Biological Sciences*, *237*(641), 37, 1952.
- Turk, G., Generating textures on arbitrary surfaces using reaction-diffusion, *Computer Graphics*, *25*(4), 289, 1991.
- Tyvand, P. A., Bladärer hos planter: Orden eller kaos?, *ORIGO*, *69*, 27, 2000.
- Weissenberger, J., Die Lebensbedingungen in den Solekanälchen des antarktischen Meereises (the environmental conditions in the brine channels of antarctic sea-ice), *Ber. Polarforschung*, *111*, 1, 1992.
- Weissenberger, J., G. G. R. Dieckmann, and M. Spindler, Sea ice: A cast technique to examine and analyze brine pockets and channel structure, *Limnol. Oceanogr.*, *37*(1), 179, 1992.
- Worster, M. G., and J. S. Wettlaufer, Natural convection, solute trapping, and channel formation during solidification of saltwater, *J. Phys. Chem. B*, *101*, 6132, 1997.

B. Kutschan, (kutschan@gmx.de)

K. Morawetz, (morawetz@physik.tu-chemnitz.de)

S. Gemming, (s.gemming@fz-rossendorf.de)